Batteries & Supercaps

Research Article
doi.org/10.1002/batt.202400721

Chemistry Europe
European Chemical Societies Publishing

www.batteries-supercaps.org

Direct Powder Adhesion Method of Quinone-Based Aqueous Supercapacitor for Roll-to-Roll Process

Nagihiro Haba,[a] Yuto Katsuyama,*[b] Ayaka Kido,[a] Keisuke Morimoto,[a] and Yuta Nakayasu*[a]

Quinone-based supercapacitors have been a growing research target as the next generation energy storage due to their high energy density and their environmental sustainability. However, the commercialization of these organic supercapacitors remains challenging due to complex fabrication processes and insufficient electrochemical performance. In this study, we introduce a novel fabrication method, direct powder adhesion (DPA), which simplifies electrode production while enhancing rate performance. Compared to conventional multi-step pressing methods, the DPA technique produces electrodes with lower density (0.48 g cm^{-3} vs. 0.52 g cm^{-3}) and significantly improves conductivity (0.74 Ω cm vs. 1.98 Ω cm). Electrochemical testing of quinone-impregnated electrodes demonstrates a high specific capacity of 217 mAh g^{-1} at 0.5 C. The DPA method demonstrated 3.5 -fold increase in the specific capacity at 5 C compared to the conventional method, showing high reversibility at higher C rates. Even when the electrode was scaled up by more than >8 times to a more practical size, the same specific capacity of 217 mAh g^{-1} at 0.5 C was achieved, demonstrating excellent scalability. Despite some challenges with high overpotential at higher rates, this study takes a significant step toward the mass production of high-performance organic supercapacitors.

Introduction

Quinone-based electrochemical capacitors have emerged as promising candidates for next generation supercapacitor.[1,2] Most commercial supercapacitors store energy by accumulating charges on high-surface-area electrode, forming an electrochemical double-layer with the cations and anions of the electrolyte. While Li-ion batteries (LIBs) dominate the current energy storage market due to their high energy density, their power density has not satisfied the market demand.[1,3] Furthermore, concerns about fire and explosion risks, as well as the environmental sustainability of rare metals, raise questions about the long-term sustainability of these batteries in mass production and consumption.[3–5]

Alternative energy storage devices that are both environmentally friendly and capable of delivering high energy and power densities are being explored. Enhancements in the energy density of current supercapacitors have been reported with the introduction of quinones.[1,2,6–11] Two ketone groups in quinones enable fast redox reaction with protons in an aqueous electrolyte, increasing the number of energy storing sites within the electrode.[12] Additionally, quinones consists of light elements, leading to a low molecular weight per redox reaction site. As a result, the weight capacity of quinone-based supercapacitors, achieving 496 mAh g^{-1} at the highest,[3] meeting the growing demand for high-power and high-energy-density supercapacitors. Despite their promising attributes, the commercialization of organic supercapacitors is still unrealized, primarily due to their inadequate electrochemical performance and high production costs. While these devices have yet to outperform conventional inorganic-based materials, ongoing advancements in material development and fabrication processes are gradually narrowing the gap.[2,7,11,13–16]

Conventional energy storage devices, including LIBs and supercapacitors, primarily use slurry casting (SC) for electrode fabrication. This method involves dispersing active materials, conductive additives, and binders in a solvent to form a slurry. Although SC is suitable for large-scale production, it poses significant challenges, especially for advanced electrode designs.[17,18] For organic supercapacitors, organic molecules are typically supported on carbon electrodes using wet processing techniques.[15,19,20] However, the drying process is highly energy-intensive, accounting for over 50 % of total energy consumption in a certain production line.[21] Solvent evaporation during drying often leads to uneven components distribution, compromising the structural and electrochemical stability of the electrodes.[17] The fabrication of thick, mechanically robust electrodes remains particularly challenging, thereby impeding efforts to enhance energy density.[22] Additionally, the widespread use of toxic organic solvents like N-methylpyrrolidone (NMP) introduces environmental risks and necessitates costly recovery systems.[18] These issues are particularly critical for

[a] N. Haba, A. Kido, K. Morimoto, Dr. Y. Nakayasu
Frontier Research Institute for Interdisciplinary Sciences, Tohoku University, 6-3 Aoba, Aza, Aramaki, Aoba-ku, Sendai, Miyagi 980-8578,
E-mail: nakaysu@tohoku.ac.jp

[b] Dr. Y. Katsuyama
Department of Chemistry & Biochemistry
University of California Los Angeles, Los Angeles, California 90095-1569,
E-mail: yutok8@g.ucla.edu

Supporting information for this article is available on the WWW under https://doi.org/10.1002/batt.202400721

Research Article
doi.org/10.1002/batt.202400721
Chemistry Europe
European Chemical Societies Publishing

supercapacitors, which require high cycle stability and rapid charge-discharge performance.

To address these challenges, transitioning from wet to solvent-free or dry processing methodologies for supercapacitor electrode production is becoming imperative. In our previous study, it was demonstrated that a stainless steel (SUS) mesh could replace a gold (Au) mesh as a current collector without introducing overpotential at 0.5 V vs Ag/AgCl during chloranil redox reactions. Using this approach, a high-voltage aqueous supercapacitor (>6 V) capable of charging a smartphone at a 1 C rate was successfully developed.[17] In this previous study, a conventional dry fabrication method,[3,7,8,11,23–25] commonly employed in the preparation of supercapacitor and battery electrodes, was utilized. This process involves pressing electrode paste multiple times after mixing it with polytetrafluoroethylene (PTFE) to ensure uniform distribution and robust connections within the electrode. The paste is then adjusted for width and thickness using a heat-stretching machine and stretched onto a SUS mesh for final preparation. However, this multi-step process is unsuitable for mass production due to its complexity and the frequent occurrence of cracks in the electrode paste. Thus, a streamlined method compatible with roll-to-roll processing is needed.

In this study, a novel direct powder adhesion (DPA) method is proposed as a single-step electrode fabrication method that can be incorporated into roll-to-roll configuration, as shown in Figure 1. The DPA method produces electrodes with higher porosity due to reduced pressing, which in turn improves rate capability compared to the conventional method which required multiple pressing steps. This study compares the material properties of electrodes fabricated using the conventional and the DPA method, followed by practical-sized half-cell tests to evaluate their performance.

Results and Discussion

Material Characterization of the Electrodes Prepared by the DPA Method

2.0 cm×2.0 cm electrodes were prepared using the quinone-impregnated carbon powder via both the conventional and the DPA method. We measured the thickness of each sample, and the electrical resistance was measured by a multimeter with 3 measurement points on each sample. Figure 2(a) shows the density as well as the electrical resistance for the 3 points on each sample. The average thickness and density of each electrode prepared by the conventional method and the DPA method were 0.61 mm and 0.52 g cm^{-3}, and 0.67 mm and 0.48 g cm^{-3}, respectively. The average electrical resistance with the 3 measuring points were 1.98 Ω cm and 0.74 Ω cm, respectively. Almost no decrease in density (0.52 to 0.48 g cm^{-3}) but a huge improvement in electrical resistance (1.98 to 0.74 Ω cm) were observed for the electrode prepared by the DPA method, compared to the electrode prepared by the conventional method. Furthermore, the conventional method demonstrated a larger error bar range of 0.76 Ω cm compared to 0.33 Ω cm for the DPA method, which indicates that the DPA method is a more consistent production method compared to the DPA method. To further investigate sample differences between these two methods, SEM images were taken for each of the samples. (Figure 2(b–e), Figure S1(a–o)) As seen in Figure 2(c), the conventional method forms internal cracks in the multiple stretching and pressing process, leading to uneven contact throughout the electrode and higher electrical resistance. Another factor is the decrease in particle size in the grinding process via coffee mill for the DPA method. As observed in Figure 2(b–e), particles with sizes of 5–15 μm are interconnected in a three-dimensional structure in the DPA method. However, in the conventional method, particles with sizes of 5–50 μm are stretched in a two-dimensional structure. The decrease in particle size increases the connecting surface areas and decreases internal resistance leading to a lower overall resistance of the electrode.[26] Porosity also plays an important role in electrochemical properties. As demonstrated in Figure 2(b, d), electrode prepared by the conventional method

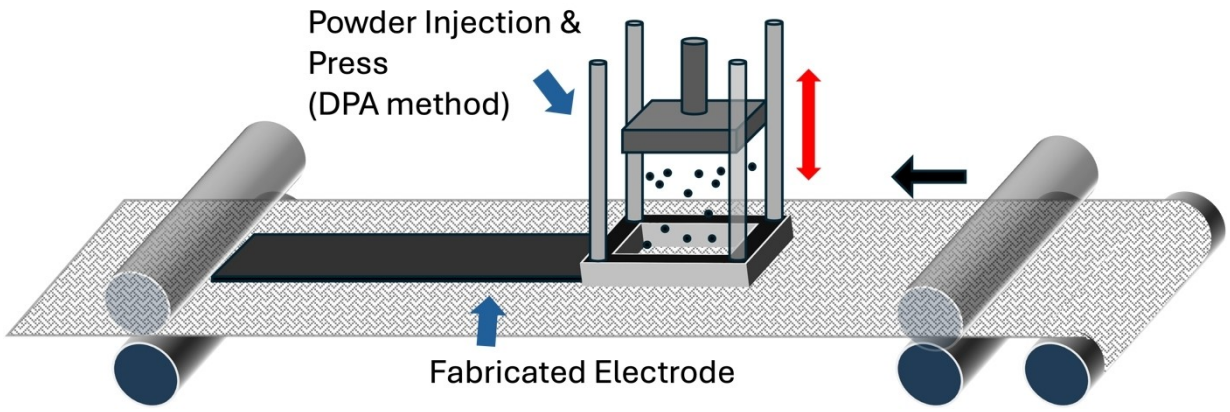

Figure 1. Concept of a Roll-to-Roll Process using the novel DPA method.

Research Article
doi.org/10.1002/batt.202400721
Chemistry Europe
European Chemical Societies Publishing

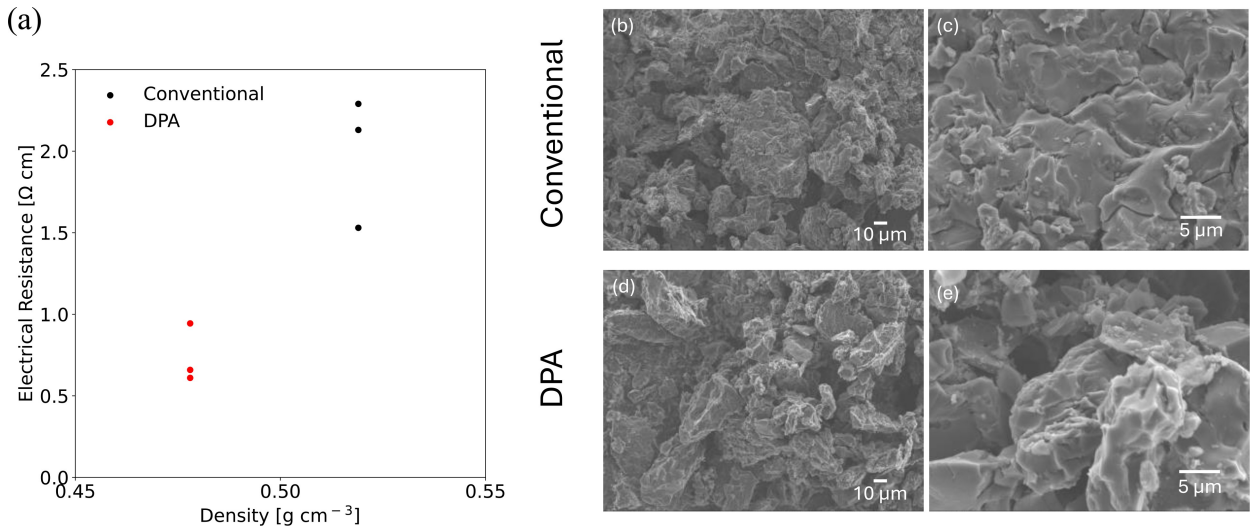

Figure 2. (a) Density versus Electrical Resistance of the sample prepared by the conventional method and DPA method. SEM image of the sample surface prepared by the conventional method taken at (b) ×500, (c) ×3000 and the sample surface prepared by the DPA method taken at (d) ×500, (e) ×3000.

showed less bumped surface morphology with fewer macro pores (>3 μm). On the other hand, electrode fabricated with the DPA method has more macro pores between the secondary particles, as shown in the figure. This plays an important role in how the electrolyte sink into the electrode, and how ions transport within the electrode.[27,28]

Electrochemical Performance

The electrodes pressed on SUS316 mesh current collectors were put into the beaker with a polypropylene separator and a counter electrode made of activated carbon (>5 times the weight of the working electrode). The electrodes were soaked in a 5 M sulfuric acid aqueous solution and vacuumed for >15 min to get rid of air bubbles inside the electrode. Electrochemical measurement was conducted using this beaker cell with an Ag/AgCl (3 M KCl) reference electrode. Figure 3(a, b) compares the charge and discharge profiles of the samples prepared by the DPA method. The mass loadings were 17 mg cm^{-2} and 33 mg cm^{-2}, respectively for Figure 3(a, b). The capacity in charge of the redox reaction of the quinone was calculated based on the charge and discharge profiles, which is defined as "redox capacity." The detail of this method is described in our previous report.[23] The obtained specific redox capacity was plotted against the cycle number in Figure 3(c, d). For a lower mass loading of 17 mg cm^{-2}, DPA and conventional method achieved a high average specific capacity of 217 and 212 mAh g$^{-1}_{\text{Quinone}}$ at 0.5 C, respectively, and both methods kept a high specific capacity of over 200 mAh g$^{-1}_{\text{Quinone}}$ until 5 C. Considering that the theoretical capacity of chloranil is 218 mAh g^{-1}, almost all of the impregnated quinone molecules were utilized for energy storage for both methods. On the other hand, for a higher-mass-loading electrode (33 mg cm^{-2}), the DPA method achieved a high specific capacity of 217 mAh g$^{-1}_{\text{Quinone}}$ at the initial 0.5 C, while the conventional method showed 205 mAh g$^{-1}_{\text{Quinone}}$. Also, high capacities were retained for the DPA method at higher rates: 83.4% retention at a 5 C and 73.7% retention at a 10 C, respectively, while the conventional method retained 30.2% at a 5 C and 0% at a 10 C. The rate performance results were summarized in a different way in the Supporting Information (Figure S2), highlighting how different the rate capabilities are at each mass loading for both methods. To compare the improvement of our method to other similar reports using conventional method fabrication, the discharge capacity with the theoretical capacity was summarized in Table S2. The improvement in rate performance as well as the overall usage of the impregnated quinone molecules could be attributed to its high electrical conductivity and the higher porosity for the better ion transport within the electrodes. However, a significant overpotential of 0.1 V was observed at a 5 C rate, which necessitates further optimization to enhance performance at higher rates for practical applications.

Practical-Sized Half-Cell Test

A more practical half-cell test was performed on a bigger sized electrode with a total electrode weight of >1 g for the working electrode. This electrode was fabricated by aligning 8 of the same 2 cm×2 cm electrodes on a larger SUS316 mesh (10 cm×10 cm). The electrode (without the current collector) had a total weight of 1.129 g with an average density of 34 mg cm^{-2} which is comparable to that of the smaller battery with 33 mg cm^{-2}. Considering that the working electrode weight in the previous sections were ~0.13 g, the electrode used in this test had ~8.5 times more weight. This electrode was put into the beaker with a polypropylene separator and a counter electrode made of activated carbon (>5 times the weight of the working electrode). Then, it was soaked in a 5 M sulfuric acid aqueous solution and vacuumed for >15 min to

Research Article
doi.org/10.1002/batt.202400721
Chemistry Europe
European Chemical Societies Publishing

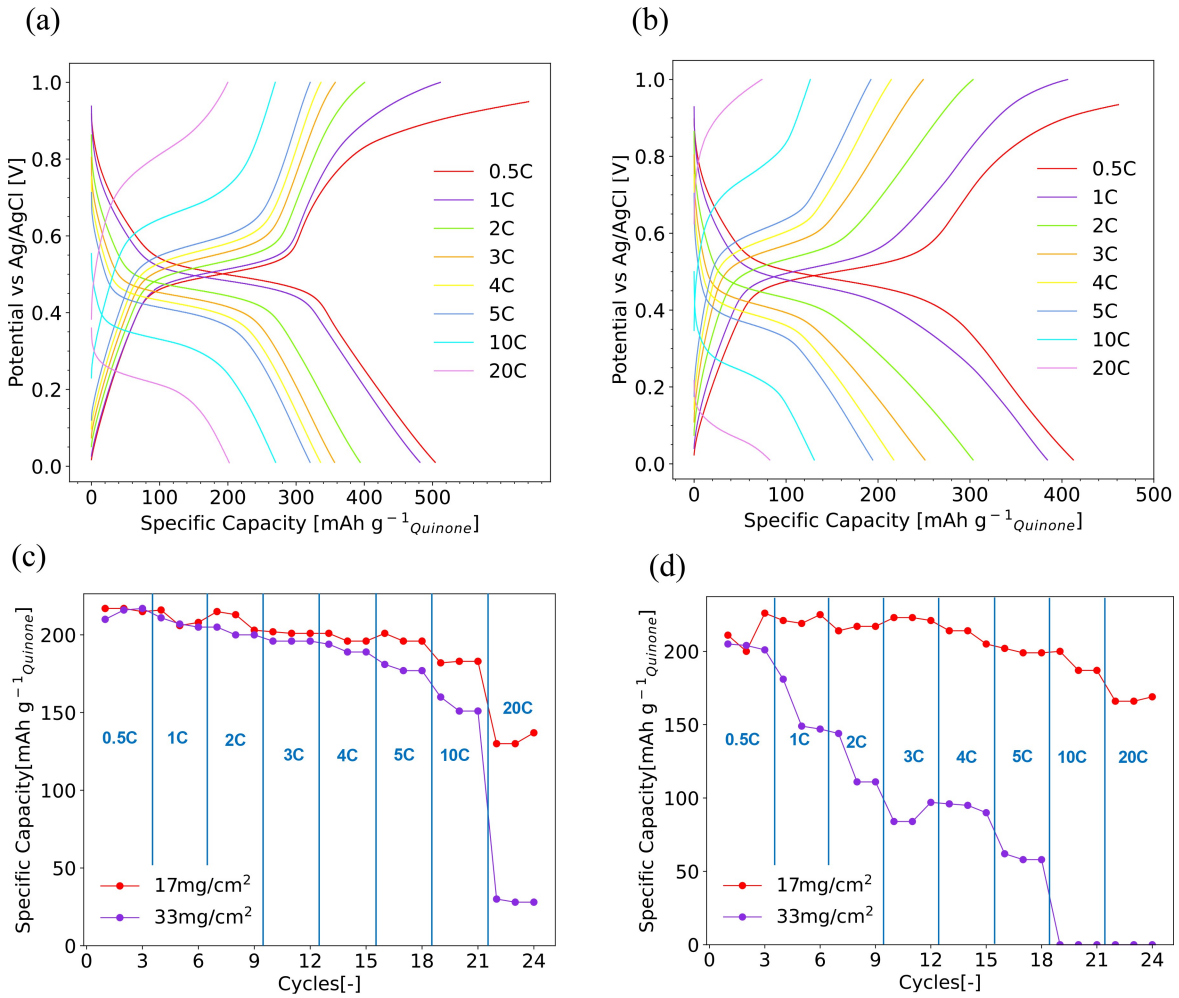

Figure 3. Charge and Discharge profiles at 0.5 to 20 C rates of the electrodes prepared by the DPA method with two different mass loadings of (a) 17 mg cm^{-2} and (b) 33 mg cm^{-2}. The cycle number vs. specific capacity plot for 17 mg/cm^2 and 33 mg/cm^2 prepared by (c) the DPA method and (d) the conventional method.

get rid of air bubbles inside the electrode. Electrochemical measurement was conducted using this beaker cell with an Ag/AgCl (3 M KCl) reference electrode. Figure 4(a) shows the charge and discharge profiles of the larger cell from 0.5 C to 5.0 C. A

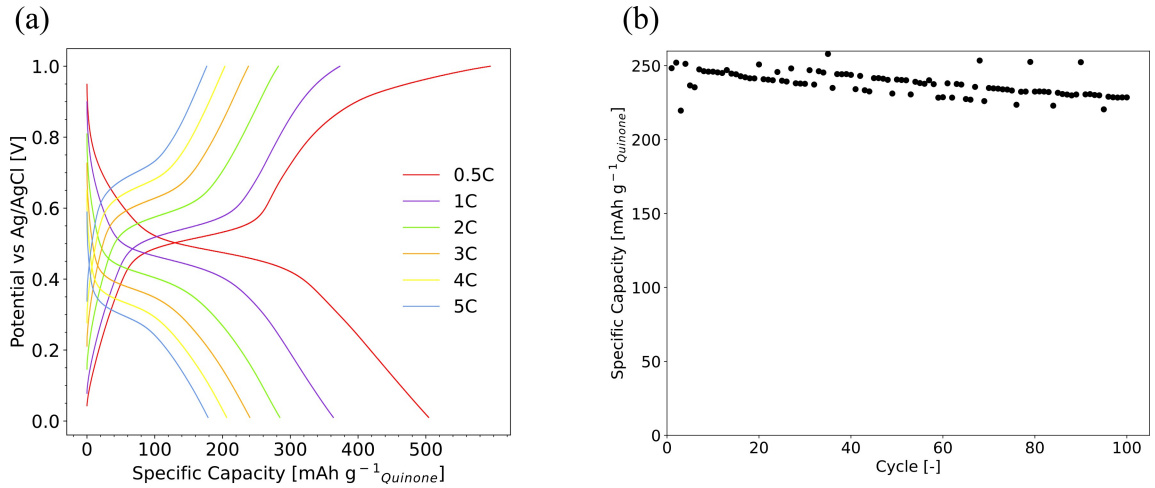

Figure 4. (a) Charge and Discharge profiles from 0.5 to 5 C rates for a larger electrode (>1 g). (b) Plots of cycle number vs. Capacity retention rate for a 1 C cycling test.

high specific redox capacity of 217 mAh g^{-1} and 210 mAh g^{-1} at 0.5 C and 1 C, respectively, were achieved. This corresponds to that of smaller electrodes, demonstrating the scalability of the DPA method. However, compared to the smaller cell in Figure 3(b), a faster increase in overpotential can be observed as it reached an overpotential of 0.1 V at a 3 C instead of a 5 C. This is due to the increase in contact resistance at the current collector-electrode interface. In a practical-sized electrode, repeated operations of up to 8 times performed on the smaller-sized electrode is necessary. During each pressing process, adjacent electrode sheets may deform, potentially leading to unstable contact with the current collector, even if it does not completely detach from it. A larger-sized mold and pressing machine could prevent this multi-step process causing the increase in contact resistance at the interface, which is one important factor in actual application.[29] To investigate the cycling capability of this battery, a cycling test was performed at a 1 C. The obtained specific capacities were plotted against cycle numbers in Figure 4(b). 92% of the initial specific capacity was maintained after 100 cycles, which is not good as reported supercapacitors. Especially, in our previous report where we used the same material, a single cell of the practical sized electrode presented 101.1% of the capacity retention rate after 100 cycles at 1 C rate.[11] The difference between the electrode made with the DPA method and the electrode fabricated in our previous report is the degree of contact at the electrode-current collector interface. As mentioned above, in the multi-step process for practical-sized electrode, electrode sheets are slightly deformed leading to uneven contact at the surface. As observed in Figure 4(b), some cycles exhibit a higher capacity retention than the rest of the cycles at around 100% which indicates a higher capacity retention when the degree of contact is fixed and all the active quinones are involved in the redox reaction. This could be achieved through fabrication of bigger and smoother mold fabricated specifically for practical sized electrodes.

Conclusions

This is the first study to optimize the fabrication method for quinone-impregnated organic supercapacitor for mass-production. In most fundamental research, the quinone-based electrode is pressed multiple times to make it flat and stretched multiple times to adjust the thickness. It is not only an industry-unfriendly method but also can cause battery failure due to cracks in the electrode and too stretched current collectors. In this research, a new method called Direct Powder Adhesion method which does not only simplify the fabrication process but also increase the porosity and electric conductivity leading to better electrochemical performance was developed. The quinone-based cathode achieved a high specific capacity of 217 mAh g$^{-1}_{\text{Quinone}}$ that matches the theoretical capacity and maintained 83.4% and 73.7% specific capacity even at high rate of 5 C and 10 C, respectively. This improvement in specific capacity compared to that of the conventional method of 205 mAh g$^{-1}_{\text{Quinone}}$ is attributed to the high electric conductivity and the porosity of the electrode. In a practical-sized battery, a high specific capacity of 217 mAh g^{-1} was achieved at 0.5 C, matching the smaller electrode. This demonstrated the scalability of the DPA method. Although some material improvements toward lower overpotential needs to be made to use organic supercapacitors at high rates, this study has taken a huge step toward mass-production and industrial application.

Methods

Material Preparation

2.04 cm×2.04 cm plastic mold was printed using PolyLite™ PLA filament purchased from Sunstella Co., Ltd, via the 3D-printer (Fusion Technology Co., Ltd, L–DEVO F300TP Plus). The mold was adjusted so that at least one side of the 2 cm×2 cm (±0.25 cm) acrylic block, purchased from Sakura Plastics Co., Ltd, fit the mold. Chloranil was purchased from Tokyo Chemical Industry Co., Ltd., activated carbon (MaxSorb®) was purchased from Kansai Coke and Chemicals Co., Ltd., stainless steel (SUS316) mesh sheet was purchased from Clever Co., Ltd., SUS316 wire was purchased from The Nilaco Co., Ltd., acetone and sulfuric acid were purchased from Wako & Co., Ltd., carbon black (VULCAN XC-72) was purchased from Full Cell Earth, Polytetrafluoroethylene (6-J) was purchased from Chemours-Mitsui Fluoroproducts Co., Ltd., Separator (MPF30AC-100) was purchased from Nippon Kodoshi Co.

Quinone Impregnation

Chloranil (0.3 g) were dissolved in 100 mL of acetone and sonicated for 10 min until it fully dissolves. Activated Carbon (0.7 g) and carbon black (0.12 g) were dispersed in the solution via sonication for 1 h. The solution was stirred at 80 °C to evaporate acetone, and impregnate quinones into the pores of the activated carbon. The obtained powder was mixed with a PTFE binder at a weight ratio of 19:1 via a mortar and pestle to form a pellet. Therefore, the weight ratio of the electrode is as follows; quinone: activated carbon: carbon black: PTFE = 25.5:59.5:10:5. Then the pellet was grinded into a powder with 300 W coffee grinder (BESROY®) for ~10 seconds.

Fabrication of Electrochemical Test Cells

For the conventional method,[12] the quinone-impregnated activated carbon powder was pressed at 30 kN by the heat press machine (As One Co., Ltd.) to form pellet electrodes. To make sure that the density on the inner and the outer side are the same, it was pressed once or twice more after the edges were bent inside. Then it was stretched to the thickness of 1.2 mm by a thermal extension device (Imoto Machinery Co., Ltd.) at 60 °C. This pellet was cut into 2 cm×2 cm size and stretched on a SUS316 mesh sheet using the same thermal extension device to the thickness of 1.0 mm to stick the pellet and SUS316 mesh sheet together.

For the DPA method, the impregnated activated carbon powder was weighed and poured evenly on a SUS316 mesh sheet inside of the mold. Then, the acrylic block was hand-pressed for a temporary connection between the mesh and the powder. The powder was then pressed at 30 kN using the heat press machine. For practical sized cells, the DPA method was repeated 8 times on a larger SUS316 mesh sheet.

The electrochemical test was operated in a half-cell configuration: Ag/AgCl (3 M KCl aq.) was used as a reference electrode, and an

excess amount (> 5 times the weight of the working electrode) of activated carbon electrode (activated carbon: PTFE = 9 : 1) was used as the counter electrode. The SUS316 mesh sheet current collectors were welded to SUS316 wires. The working electrodes and the counter electrodes were separated using a polypropylene separator (Nippon Kodoshi Co.) in a beaker cell and the 0.5 M H_2SO_4 aqueous solution was used as the electrolyte. This beaker was vacuumed for 30 min to remove the gas from the pores of the electrode.

Electrochemical and Characterization Test

A potentiostat (Ivium, Vertex) was used for electrochemical measurements. The voltage range for the charging and discharging test was 0.01 to 1.0 V and the C rates were calculated based on the theoretical capacity of the chloranil. The electrode width was measured with a slide caliper (Mitutoyo Corp., CD-15AX). Electrical resistance measurement was performed via the multimeter (Nitto-seiko, MCP–T380). The surface morphology of the electrodes was analyzed by Scanning Electron Microscope (JEOL, JSM-6500F).

Acknowledgements

This study was financially supported by the Japan Society for the Promotion of Science (JSPS) KAKENHI [grant number 24K01243], the Frontier Research Institute for Interdisciplinary Sciences (FRIS), Tohoku University, and the Tohoku Initiative for Fostering Global Researchers for Interdisciplinary Sciences (TI-FRIS) of MEXT's Strategic Professional Development Program for Young Researchers. Generous support from the FRIS CoRE, Tohoku University, which is a shared research environment, is also acknowledged.

Conflict of Interests

The authors declare no conflict of interest.

Data Availability Statement

The data that support the findings of this study are available from the corresponding author upon reasonable request.

Keywords: Carbon · Mass loading · Organic battery · Supercapacitor · Quinones

[1] S. P. Ega, P. Srinivasan, *J. Energy Storage* **2022**, *47*, 103700.
[2] Y. Zhou, Q. Wei, L. Xiao, C. Meng, Q. Yin, S. Song, Y. He, R. Qiang, Y. Yang, Z. Li, Z. Hu, *Energy Fuels* **2024**, *38*, 7399–7411.
[3] J. Bitenc, T. Pavčnik, U. Košir, K. Pirnat, *Materials* **2020**, *13*, 506.
[4] Y. Chen, Y. Kang, Y. Zhao, L. Wang, J. Liu, Y. Li, Z. Liang, X. He, X. Li, N. Tavajohi, B. Li, *J. Energy Chem.* **2021**, *59*, 83–99.
[5] B. L. Diaz, X. He, Z. Hu, F. Restuccia, M. Marinescu, V. J. Barreras, Y. Patel, G. Offer, G. Rein, *J. Electrochem. Soc.* **2020**, *167*, 090559.
[6] X. Chen, H. Wang, H. Yi, X. Wang, X. Yan, Z. Guo, *J. Phys. Chem. C* **2014**, *118*, 8262–8270.
[7] N. Tisawat, C. Samart, P. Yaiyong, R. A. Bryce, K. Nueangnoraj, N. Chanlek, S. Kongparakul, *Appl. Surf. Sci.* **2019**, *491*, 784–791.
[8] T. Tomai, H. Saito, I. Honma, *J. Mater. Chem. A* **2017**, *5*, 2188–2194.
[9] D. M. Anjos, J. K. McDonough, E. Perre, G. M. Brown, S. H. Overbury, Y. Gogotsi, V. Presser, *Nano Energy* **2013**, *2*, 702–712.
[10] M. Zeiger, D. Weingarth, V. Presser, *ChemElectroChem* **2015**, *2*, 1117–1127.
[11] Y. Katsuyama, Y. Nakayasu, K. Oizumi, Y. Fujihara, H. Kobayashi, I. Honma, *Adv. Sustainable Syst.* **2019**, *3*, 1900083.
[12] T. Tomai, S. Mitani, D. Komatsu, Y. Kawaguchi, I. Honma, *Sci. Rep.* **2014**, *4*, 3591.
[13] M. Khalid, A. Hassan, A. M. B. Honorato, F. N. Crespilho, *J. Electroanal. Chem.* **2019**, *847*, 113193.
[14] D. Malka, O. Hanna, T. Hauser, S. Hayne, S. Luski, Y. Elias, R. Attias, T. Brousse, D. Aurbach, *J. Electrochem. Soc.* **2018**, *165*, A3342.
[15] K. Lee, J. Hwang, J. H. Park, J. Park, K. Lee, J. M. Ko, *Macromol. Res.* **2023**, *31*, 171–179.
[16] Y. Nakayasu, S. Sokabe, Y. Hiraga, M. Watanabe, *Chem. Commun.* **2023**, *59*, 3079–3082.
[17] Y. Li, Y. Wu, Z. Wang, J. Xu, T. Ma, L. Chen, H. Li, F. Wu, *Mater. Today (Kidlington)* **2022**, *55*, 92–109.
[18] J. Liu, B. Ludwig, Y. Liu, Z. Zheng, F. Wang, M. Tang, J. Wang, J. Wang, H. Pan, Y. Wang, *Adv. Mater. Technol.* **2017**, *2*, 1700106.
[19] Q. Zhao, W. Huang, Z. Luo, L. Liu, Y. Lu, Y. Li, L. Li, J. hu, H. Ma, J. Chen, *Sci. Adv.* **2018**, *4*, eaao1761.
[20] Z. Lin, H. Shi, L. Lin, X. Yang, W. Wu, X. Sun, *Nat. Commun.* **2021**, *12*, 442422.
[21] K.-H. Pettinger, W. Dong, *J. Electrochem. Soc.* **2017**, *164*, A6274.
[22] J. Liu, B. Ludwig, Y. Liu, Z. Zheng, F. Wang, M. Tang, J. Wang, J. Wang, H. Pan, Y. Wang, *Adv. Mater. Technol.* **2017**, *2*, 1700106.
[23] Y. Katsuyama, T. Takeyuki, S. Sokabe, M. Tanaka, M. Ishizawa, H. Abe, M. Watanabe, I. Honma, Y. Nakayasu, *Sci. Rep.* **2022**, *12*, 3915.
[24] B. Yang, Y. Ma, D. Bin, H. Lu, Y. Xia, *ACS Appl. Mater. Interfaces* **2021**, *13*, 58818–58826.
[25] H. Kobayashi, K. Oizumi, T. Tomai, I. Honma, *ACS Appl. Energ. Mater.* **2022**, *5*, 4707–4711.
[26] T. Eguchi, Y. Kanamoto, M. Tomioka, D. Tashima, S. Kumagai, *Batteries* **2020**, *6*, 22.
[27] Y. Katsuyama, N. Haba, H. Kobayashi, K. Iwase, A. Kudo, I. Honma, R. B. Kaner, *Adv. Funct. Mater.* **2022**, *32*, 2201544.
[28] Y. Katsuyama, Z. Yang, M. Thiel, X. Zhang, X. Chang, C. Lin, A. Huang, C. Wang, Y. Li, R. B. Kaner, *Small* **2024**, *20*, 2305921.
[29] A. Abdisattar, Y. Mukhtar, D. Chingis, A. Kydyr, T. Aidos, T. Azamat, P. Nikolay, *Electrochem. Commun.* **2022**, *142*, 107373.

Manuscript received: November 11, 2024
Revised manuscript received: December 24, 2024
Accepted manuscript online: December 25, 2024
Version of record online: January 15, 2025